39th AIAA/ASME/SAE/ASEE Joint Propulsion Conference and Exhibit
20-23 July 2003, Huntsville, Alabama

AIAA 2003-4593

39th AIAA/ASME/SAE/ASEE Joint
Propulsion Conference and Exhibit
20 – 23 July 2003
Huntsville, AL

NANO-SIZED ALUMINUM- AND BORON-BASED SOLID-FUEL CHARACTERIZATION IN A HYBRID ROCKET ENGINE

Grant A. Risha*, Brian J. Evans**, Eric Boyer*, Robert B. Wehrman†, and Kenneth K. Kuo‡
The Department of Mechanical and Nuclear Engineering
The Pennsylvania State University
University Park, PA 16802

ABSTRACT

An experimental investigation was conducted to determine the relative propulsive and combustion behavior of various hydroxyl terminated polybutadiene (HTPB)-based solid-fuel formulations containing nano-sized energetic particles. In total, 19 solid fuel formulations were investigated. Seventeen formulations contained 13% additive, one contained 6.5%, and one contained 5.65% boron (by weight). Nano-sized particles were cast in an HTPB solid-fuel grain and burned in the Long Grain Center-Perforated (LGCP) hybrid rocket engine using pure oxygen as the oxidizer injected at the head-end of the engine. The addition of nano-sized particles into the solid fuel significantly enhanced performance due to the short ignition (~4 ns) and combustion times (~50 ns) and higher heat release near the surface. It was found that the addition of 13% energetic powders (such as Viton-A coated Alex®) showed an increase of up to 120% in mass burning rate compared to the pure HTPB fuel for an average oxidizer mass flux of 112 kg/m^2-s. Chemical and physical analyses were conducted on the nano-sized energetic particles to determine the oxide layer thickness, active aluminum content, and the average particle size. Alex® particles had the highest active aluminum content of 84.6% while minimizing the oxide layer thickness to 4 nm. Viton-A coated aluminum flakes showed a mass burning rate increase of nearly 42% compared to HTPB and twice the increase compared to the uncoated flakes because fluorine and fluorine-containing compounds produced from the dissociation of Viton-A contributed to the rapid ignition and combustion. Boron-based solid fuels showed significant increase (~44%) in mass burning rate which indicates there could be higher energy feedback from the combustion zone to the regressing fuel surface due to boron's higher heat of oxidation. The effect of pressure on the liner regression rate was investigated and was verified to be independent of pressure. Nano-sized Alex® particles (13% by weight) coated with Viton-A had average η_{C^*} ranging from 88 to 92%, where the solid fuel containing micron-sized aluminum particles exhibited combustion efficiencies from 81 to 85%. The boron-containing (5.65% boron) formulation had a molar equivalence of 13% aluminum (by weight). By comparing the 13% boron formulation and the 5.65% boron formulation, it was evident that the 5.65% boron solid fuel had a higher C* combustion efficiency (83%) than the entire range (78 to 81%) for fuels containing 13% boron. The thrust level for the formulation containing Alex® particles (13% by weight) coated with Viton-A was highest among all formulations.

INTRODUCTION

Some of the earliest rocket propulsion systems employed the hybrid rocket configuration, which was then called solid-liquid rocket propulsion.[1,2] The conception of a hybrid rocket has been around since the late 1930's. Hybrid rockets are a type of chemical rocket propulsion system which employ propellant ingredients separated physically and also by phase.[1] This separation is the inherent source of safety.

Hybrid rocket propulsion systems (using solid fuels and liquid oxidizers) have many advantages over conventional solid- and liquid-propellant rockets, especially in view of the recent growing emphases on improved safety and reliability, low development cost, minimal environmental impact, on-off operational capability, and greater controllability for rocket engines.[3,4]

The fluid dynamic and combustion processes in the hybrid rocket engine are characterized by complex interactions between numerous physical phenomena simultaneously taking place in the combustion chamber, such as solid-fuel pyrolysis, oxidizer atomization and vaporization, gas-phase diffusion, mixing and combustion, turbulent flow with mass addition, convective and radiative heat transfer, and varying flow-channel configuration. The fuel-surface regression rate, which is a very important design and

* Ph.D. Candidate, AIAA Student Member
** M.S. Student, AIAA Student Member
† Undergraduate Assistant
‡ Distinguished Professor of Mechanical Engineering, AIAA Fellow

performance parameter, is strongly affected by the operating conditions in addition to the composition and thermophysical properties of the solid fuel. The effects of the reactive environment composition and pressure on the solid-fuel thermal decomposition and regression rate were of much interest to the development of performance prediction and scale-up design tools. Therefore, these effects have been the subjects of many basic studies, which reached debatable conclusions, among researchers in hybrid propulsion.

Since the combustion process of solid fuels is governed by the mass flux of the oxidizer entering the combustion chamber, the rate-limiting process of combustion in hybrid rockets is the mixing and reacting of the pyrolysis products of fuel with the oxidizer flowing through the center port of the solid-fuel grain.[5,6] Thus, the average regression rate can be correlated with the local port mass flux. The major disadvantage of the existing solid fuels is the relatively low mass burning rate for practical oxidizer mass fluxes, requiring a relatively large fuel surface area for a given thrust level. This performance can be improved using various solid-fuel performance enhancement techniques.

Solid Fuel Performance Enhancement Techniques

Several studies have been conducted to improve the regression rate of various solid fuels used in both solid fuel ramjets and hybrid rockets. The performance enhancements techniques/ingredients can be broken down into four distinct categories such as: 1) the addition of nano-sized energetic particles into the solid fuel grain; 2) coating the energetic particles to provide additional oxidizer near the reaction zone with highly-reactive polymers; 3) the substitution of the virtually inert HTPB binder with more energetic polymers (e.g. glycidyl azide polymer, GAP); and 4) the replacement of liquid oxygen (LOX) with more energetic and dense liquid oxidizers like hydroxyl ammonium perchlorate (HAP) or hydroxyl ammonium nitrate (HAN). Unfortunately, by using some of the above-mentioned ingredients, the system can be subjected to other undesirable problems such as processing issues, handling, and/or cost.

Nano-Sized Particle Additives

The inclusion of energetic materials in solid fuels provide energy enhancement as well as increased density of the solid fuel. Historically, energetic particles (such as aluminum) have been introduced in solid fuels used in ramjet applications. These particles were usually on the order of tens of hundreds of microns, with the smallest being 2-5 microns. Despite the large scale of the particles, the energy release from the oxidation of the metal particles still substantially increased the regression rates. With this apparent benefit in mind, nano-sized particles possess the ability to release the energy in a quicker, more effective manner. Thus, the low solid-fuel mass burning rate can be ameliorated by using energetic nano-sized powder additives, developed by various groups.[7,8] There are many direct advantages of incorporating nano-sized materials into fuels and propellants such as: 1) shorter ignition delay and burning time; 2) more complete combustion in volume-limited propulsion systems; 3) greater flexibility in designing new energetic fuel/propellants with desirable physical properties; and 4) act as gelling agent for liquids replacing inert or low energy gelling agents (i.e. Cab-O-Sil).

Although nano-sized particles do possess desirable characteristics, they do have some undesirable ones, too. Aluminum particles generally have an oxide layer, which makes the particle less reactive until the oxide layer is removed. For smaller particles, the oxide weight percentage increased and the solid fuel grain processing became very difficult. In previous hybrid studies conducted by the research team at PSU,[9,10] the addition of 20% Alex® powder into the HTPB fuel was found to increase the mass burning rate by 70%. This demonstrated that a very significant improvement of solid-fuel performance in hybrid engine operating conditions was achieved with ultra-fine aluminum powders. Kuo and co-workers[11] also demonstrated that Alex® particles substantially enhanced the linear burning rate of aluminized solid propellants by 100%. The results were obtained from strand burning studies of two identical propellant formulations (one with 18% regular aluminum powder and the other with 9% replacement by Alex®).

Polymeric/Metal Coatings on Nano-Sized Particles

It is well known that the ignition and boiling temperatures of boron are extremely high, which can cause difficulty for ignition. Coatings may assist in remedying this problem. Several researchers have conducted experiments to determine the effect on ignition and burning rate of boron particles using coatings containing polymers and/or other reactive materials. Li and Jin[12] studied the effects of coating sub-micron sized boron (~ 0.8 μm) with materials such as ammonium perchlorate (AP), potassium perchlorate (KP), lithium fluoride (LiF), and magnesium. They found that the coating containing either AP or KP increased the combustion temperature over 200 ^{o}C. The KP coating also increased the burning rate approximately 10%. Finally, the boron powder coated

with both KP and LiF increased the burning rate 36% in an atmospheric environment. Shyu and Liu[13] coated micron-sized boron particles (average diameter ~51 μm) with glycidyl azide polymer (GAP) and characterized combustion in the hot product gas stream of a flat-flame burner. They concluded that propellants containing GAP-coated amorphous boron particles exhibited more intense combustion characteristics, higher burning rates, and less residue agglomeration than a baseline propellant containing uncoated boron. In a subsequent study, Liu *et al.*[14] investigated amorphous boron with a mean particle diameter of 2 μm coated with LiF, vinylidine fluoride / hexafluoropropylene co-polymer (Viton-A), or silane in a ducted rocket. They found that the LiF coating performed the best in terms of combustion. Viton-A coating exhibited a slightly lower burning rate than the LiF coating and the silane coating was not effective at all. Some of the particles in the current study at PSU have been coated with Viton-A by Dr. May Chan of NAWC-China Lake.[15] Viton-A ($C_5H_{3.5}F_{6.5}$) seems to be a very promising candidate for coatings since the fluorine in the polymer (66.5% by weight) can enhance ignition and combustion of metal particles, especially particles such as boron that have an oxide coating and high ignition temperature.

Motivation and Objective

Existing solid propellant missiles have relatively low specific impulses, but high density impulses. In addition, the burning rates of the current solid propellant grains in the existing systems are limited due to the less efficient burning-rate modifiers that have been utilized in the conventional solid propellants. Several other undesirable features of the solid-propellant rocket systems are: 1) not being capable of thrust modulation; 2) the propellant grain cannot be extinguished once the grain is ignited; 3) their susceptibility to mechanical damage and subsequent flame spreading into the damaged regions and potential catastrophic motor failure; and 4) solid fuel mechanical properties are sacrificed because of relatively low loading densities. Hybrid propulsion systems utilizing solid fuel and liquid or gas oxidizer have many advantages over conventional liquid- or solid-propellant systems such as inherent safety, more environmental friendliness, and improved operability.[16] As mentioned, the major disadvantage of the existing solid-fuel grains is the relatively low mass burning rate of the fuel, requiring a relatively large fuel surface area for a given thrust level. Low burning rates of solid fuels have been shown to be enhanced by the addition of energetic metal powders.

The objective of this investigation was to characterize a family of HTPB-based high-energy solid fuels that have great potential for generating superior propulsion performance. Several types and shapes of energetic nano-sized particles have been embedded in various solid fuel grains. The types of energetic aluminum and boron materials, manufacturer, size, and geometry is given in Table 1.

METHOD OF APPROACH

Hybrid Rocket Engine Experimental Setup

The Long Grain Center-Perforated (LGCP) hybrid rocket engine was designed to allow quick fabrication of the system and rapid turn-around between test runs. A schematic of the LGCP test rig installed on the test stand is shown in Fig. 1.

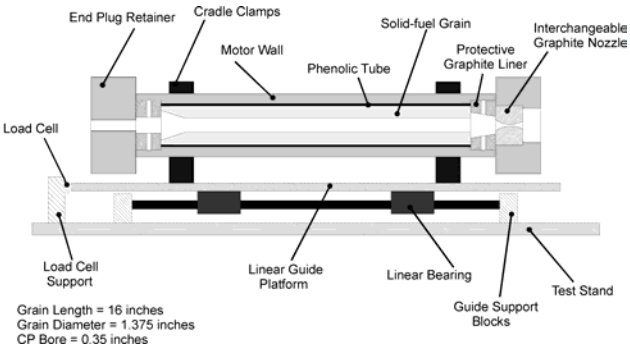

Fig. 1. Schematic diagram of LGCP hybrid engine

The engine was equipped with two Setra pressure transducers to monitor the pressure near the oxidizer injector and the exit nozzle. The engine has the capability of housing different pre-cut nozzles and fuel grains cast into phenolic tubes, with grain length up to 41 cm (16 in). The oxygen feed system of the LGCP hybrid rocket engine is capable of oxygen mass flow rates up to 0.36 kg/s (0.8 lbm/s) and chamber working pressures up to 12 MPa (1,750 psig). A 450-N (100-lb_f) load cell was used to determine the instantaneous thrust of the engine. A more detailed description of the test facility can be found in Refs. 17 and 18. For the test firings reported in this paper, the nano-sized particles were cast in an HTPB solid-fuel grain and burned in the LGCP motor using pure oxygen as the oxidizer injected at the head-end of the motor. The initial oxidizer mass flux ranged from 140 to 850 kg/m^2-s (0.2 to 1.2 lbm/in^2-s). The average chamber pressure for tests in this series ranged from 2.3 to 4.6 MPa (320 to 650 psig) and the time duration from the onset of ignition to the oxygen cutoff ranged from 5 to 7 seconds. The oxygen supply was cut off and a purge stream of nitrogen was immediately injected in the head end of the LGCP to extinguish combustion.

Table 1. Description of nano-sized particles and flakes used in this study

Nano-Sized Particles or Flakes	ID	Distributor	Average Diameter [nm]	Specific Surface Area [m^2/g]	ρ [g/cm^3]
Aluminum particles	Alex®	Argonide Corp.	100-150	13	2.70
Aluminum particles	WARP-1	CMPI	70	27.5	2.70
Aluminum flakes	SILBAL	Silberline	50-200 thick	-	2.55
Aluminum flakes w/ Viton-A coating	CLAL	NAWC-China Lake	50-200 thick	-	2.55
Aluminum particles	TECHAL	Technanogy	46	40	2.70
Boron carbide particles	B_4C	CMPI	120	13	2.60
Boron carbide w/ catalyst coating	Cat-B_4C	CMPI	120	13	2.60
SB 99% pure amorphous boron	Boron	SB Boron Corp.	< 150	31	2.34
Alex® aluminum w/ Viton-A coating	C-Alex®	NAWC-China Lake	100-150	13	2.70
Aluminum particles quenched in argon	IHD-AR	NSWC-Indian Head	80	20-30	2.70
Aluminum particles	NTECH-80	Nanotechology	80	26.5	2.70
Aluminum particles	NTECH-50	Nanotechology	50	41.7	2.70
Aluminum particles in R45 resin	AVAL	AVEKA, Inc	30-40	63	2.70
SB 99% pure amorphous boron coated w/ Viton-A	C-Boron	NAWC-China Lake	< 150	31	2.34

Solid-Fuel Processing Using Nano-Sized Materials

A detailed solid fuel processing procedure was also discussed in Refs. 16 and 17. Briefly, hydroxyl-terminated polybutadiene (HTPB) was used as the baseline solid-fuel (SF1). The nano-sized particles were introduced into the R-45HT resin (from Sartomer) and mixed for ten minutes. Subsequently, the mixture was placed in an ultrasonic bath for an additional 10 minutes to break up any agglomerations of the nano-sized particles. Finally, the polymer resin/nano-sized particle mixture was combined with a curing agent, Isonate 143L (MDI, from Dow Chemical), and mixed under vacuum for 10 minutes. Information regarding each solid-fuel formulation is shown in Table 2.

The weight percentage of the energetic additive, molecular weight, specific heat, and density of the solid fuel was given in Table 2. Indicated directly preceding the energetic additive is the weight percent of that specific material in the solid fuel formulation. The remaining weight percentage was comprised of pure HTPB and curing agent. In addition, there are two density values given. The density with the subscript "vol" is a volumetric-weighted average based on the solid fuel ingredients.

Density of the Solid Fuels

The measured density column in Table 2 was values obtained from pycnometer experiments. Since the ingredients in the solid fuel do not have the same densities, the volume occupied by a certain amount of material must be considered. Thus, the calculated density of the mixture was determined using a volumetric-weighted average as indicated in Table 2 as "vol."

The densities of the cured HTPB and aluminum are 920 kg/m^3 and 2702 kg/m^3, respectively. The measured densities agree well with the calculated values. The range of variation is from 0.3% to 2.5%, while the average variation is approximately 1.35%.

Table 2. Properties of HTPB-based energetic solid fuel formulations*

Solid Fuel	Additive (by wt%)	MW_{SF} [kg/kmol]	$C_{p,SF}$ [J/kg-K]	$\rho_{SF\text{-}meas}$ [kg/m^3]	$\rho_{SF,vol}$ [kg/m^3]
SF1	None	99.954	1633	921	920
SF2	13%Alex®	73.953	1373	986	1006
SF3	13%B_4C	90.443	1487	979	1004
SF4	6.5%WARP-1	85.010	1484	945	962
SF5	6.5% B_4C/ 6.5%WARP-1	81.371	1424	966	958
SF6	13%BORON	48.239	1281	1017	999
SF7	13%SILBAL	70.953	1373	1027	1003
SF8	13%CLAL	70.953	1373	1017	1003
SF9	13%WARP-1	73.953	1373	995	1006
SF10	13%Cat-B_4C	90.443	1487	1007	1004
SF11	13%TECHAL	73.953	1373	999	1006
SF12	13%Al-325	73.953	1373	991	1006
SF13	13%C-Alex	85.266	1373	992	1006
SF14	13%C-Boron	75.327	1281	965	999
SF15	13%AVAL	73.953	1373	1009	1006
SF16	13%IHD-AR	73.953	1373	1015	1006
SF17	13%NTECH-80	73.953	1373	998	1006
SF18	13%NTECH-50	73.953	1373	1013	1006
SF19	5.65%BORON	68.185	1371	942	953

*Tabulated values do not include the effect of trace amounts of chemical additives or oxide layers on particles

Solid Fuel Homogeneity

The homogeneity of the solid fuel containing nano-sized energetic particles was verified by two techniques: Scanning Electron Microscopy (SEM) and Energy Dispersion Spectroscopy (EDS). In the first technique, high-resolution SEM micrographs were taken of the unburned solid fuel to determine the distance between particles. The second technique, EDS, provided a map of the elements in the field of view. Both methods revealed that the solid fuel and nano-size particles were extremely well-mixed. Figure 2 shows a SEM micrograph of unburned SF2 (Alex®-containing solid fuel). The total area in the micrograph was approximately 49 μm^2. It was evident that the nano-sized particles were well dispersed in the HTPB polymer. The largest distance between particles was around 1.5 micron; however, the average distance between particles was around 250 nm.

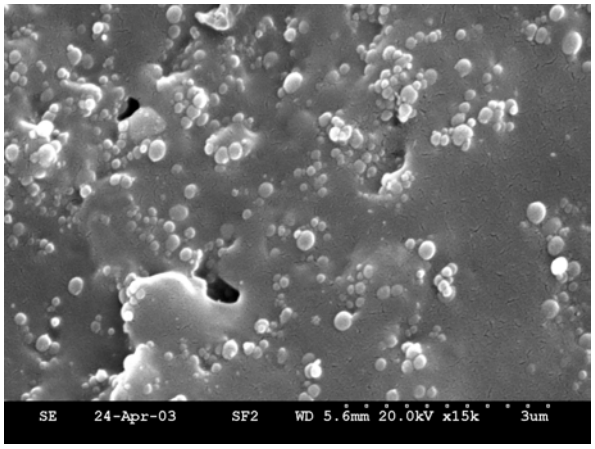

Fig. 2. SEM micrograph of unburned solid fuel containing nano-sized Alex® aluminum particles (SF2)

Figure 3 is a map of the elemental atoms detected by the EDS system. This map agreed well with the SEM micrograph in the previous figure indicating a well-mixed solid fuel. In Fig. 3, the small white dots represent the presence of oxygen, aluminum, and carbon in each corresponding window. The upper left window corresponds to aluminum and the upper right window corresponds to carbon. These two windows indicated that aluminum was present uniformly where the carbon was located which demonstrated a well-mixed condition since the polymer is 87% of the solid fuel.

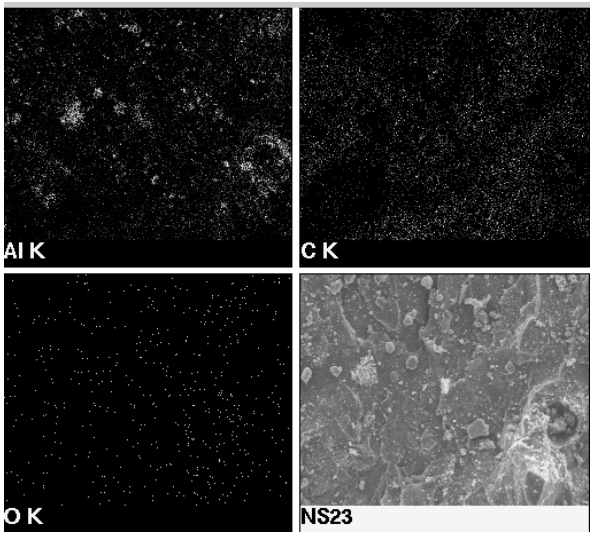

Fig. 3. EDS elemental map of unburned solid fuel containing nano-sized Alex® aluminum particles (SF2)

DISCUSSION OF RESULTS

Thirteen different types of nano-sized particles were analyzed to determine the active aluminum/boron content in the particles. Also, over 85 hybrid rocket engine test firings were conducted in the LGCP using gaseous oxygen as the oxidizer. In this investigation, 19 solid fuel formulations have been studied. Seventeen formulations have 13%, one (SF4) has 6.5%, and one (SF19) has 5.65% of a specific energetic additive.

Active Aluminum Content

According to Johnson and Higa[19] in an earlier paper, the oxide layer around the (assumed) spherical Alex® particle obtained from the Argonide Corporation was 3.68 nm; this implied that the weight percentage of active aluminum is 79.1%. In this investigation, the active aluminum content was determined by employing two methods: Thermogravimetric Analysis (TGA) and base hydrolysis.

The amount of mass gained due to the aluminum oxidation process was determined. In this analysis, it was assumed that the available aluminum in the sample undergoes complete oxidation. Therefore, the mass added to the sample during oxidation is exclusively a result of oxygen reacting with the aluminum. Knowing the stoichiometric ratio and the amount of oxygen that was gained during oxidation, the amount of active (non-oxidized) aluminum originally in the sample can be determined.

The base hydrolysis method was performed by Dr. Curtis C. Johnson of NAWCWD, China Lake, CA.[20] The sample was placed into an aqueous solution of potassium hydroxide (KOH) to determine the amount of active aluminum in a nano-particle. The neat aluminum material reacted to form $Al(OH)^-_4$ and generates hydrogen gas. The higher the active aluminum in the sample, the greater amount of hydrogen produced. The quantity of hydrogen was measured and ultimately compared to the hydrogen amount generated from a known standard (Valimet H-2 aluminum powder). These experiments yielded results with 2% accuracy. A summary of the active aluminum content for each nano-sized particle type is given in Table 3. Silberline reports that the aluminum oxide layer on their flakes was less than 1% oxide (by weight).[21] The CLAL aluminum flakes are coated Silberline with 10% Viton-A by Dr. May Chan of NAWC-China Lake.

Table 3. Summary of active aluminum/boron content in nano-sized particles used in this study

Particle/Flake	Active Al or B (wt%) KOH Hydrolysis	TGA
Alex®	84.8	84.4
SILBAL	88.8	86.2
TECHAL	58.1	67.2
CLAL	61.8	69.0
WARP-1	49.2	51.0
C-Alex®	N/A	78.8
AVAL	N/A	33.5
IHD-Ar	N/A	76.3
IHD-He	N/A	43.9
NTECH-50	N/A	61.0
NTECH-80	N/A	74.0
Boron	N/A	74.7
C-Boron	N/A	74.7
Valimet H-2	98.6	N/A

Lab-Scale Rocket Engine Tests

A typical pressure-time trace from LGCP test firing is given in Fig. 4. In this case, the solid fuel contained 13% boron.

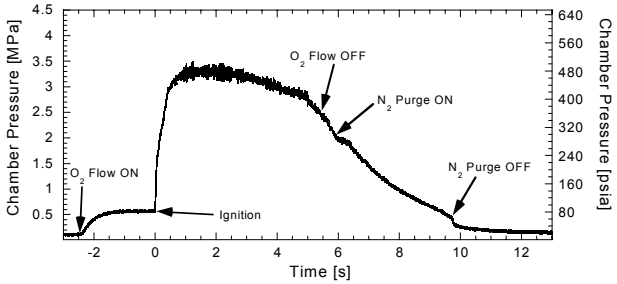

Fig. 4. Typical P-t trace of LGCP hybrid rocket firing using SF6

The oxygen flow was initiated approximately 2 seconds before the igniter was triggered in order to obtain a steady-state oxidizer flow condition to enhance ignition. After a certain period of time, the oxidizer flow was shut off followed by the onset the nitrogen purge to stop combustion and cool the chamber components. The chamber pressure was not entirely constant during the run. The pressure was slightly decreasing which was due to the reduction of the oxidizer mass flux as the port enlarges. In Fig. 5, the mass-burning rate was correlated with the average oxidizer mass flux using a conventional power law shown in Eq. (3).

$$\dot{m}_b \left[{}^{kg}/_{s} \right] = A \cdot \left[G_{ox,ave} \left({}^{kg}/_{m^2-s} \right) \right]^n \qquad (3)$$

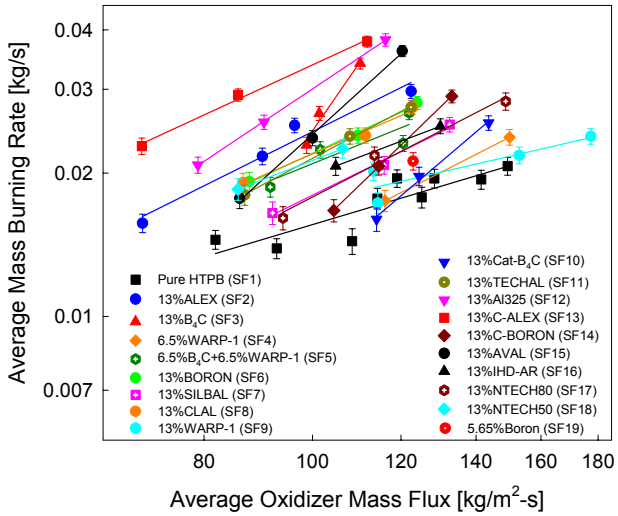

Fig. 5. Comparison of mass burning rate correlations for various solid-fuel formulations

where $G_{ox,ave}$ is the average oxidizer mass flux and A is the pre-power factor. In addition, Fig. 6 shows the average regression rate correlated with a similar power law functional form in Eq. (4). The power-law curve-fit parameters for Eqs. (3) and (4) are given in Table 4 for all of the solid-fuel formulations studied.

$$r_b\left[{}^{mm}/_{s}\right] = B \cdot \left[G_{ox,ave}\left({}^{kg}/_{m^2-s}\right)\right]^m \qquad (4)$$

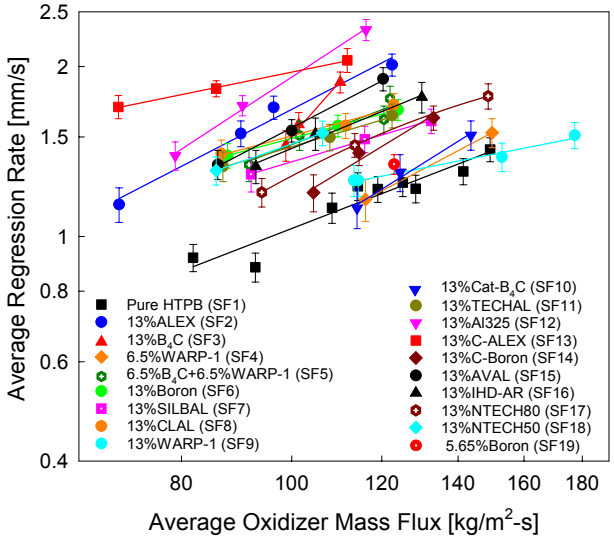

Fig. 6. Comparison of linear regression rate correlations for various solid-fuel formulations

As shown in Fig. 5, the baseline solid fuel (SF1) demonstrated the lowest mass-burning rate. SF3 showed a significant slope increase compared to other solid fuel formulations. This was a result of non-uniform burning of the solid fuel grain. Large "ditch-like" canals were observed in the solid fuel web after the test firing. It is evident from Fig. 5 that virtually all of the curve fits for each corresponding solid fuel formulation exhibit a divergence in the average mass burning rate compared to the baseline solid fuel formulation (SF1) indicating that as the average oxidizer mass flux was increased, the mass-burning rate compared to the baseline continually increased. SF12 and SF13 appeared to have the highest average mass-burning rate. Among all formulations, SF12 was the only solid fuel formulation which contained micron-sized particles. This was intended to provide a comparison of the performance parameters between nano-sized and micron-sized particles. SF5, SF6, SF8, and SF11 appear to have very similar average mass-burning rates although each formulation contained different energetic materials.

SF1 (pure HTPB) demonstrated the lowest average linear regression rate. Similar to the mass burning rates, SF12 and SF13 also had the highest linear regression rates. The slope of SF13 was much less than that of SF12; hence, the performance was less affected

Table 4. Power-law correlation parameters for mass burning rate and linear regression rate for all solid fuels[22]

Solid Fuel	Mass Burning Rate Parameters		Linear Regression Rate Parameters	
	A [kg/s]	n	B [mm/s]	m
SF1	89.960×10^{-5}	0.627	0.05410	0.647
SF2	11.111×10^{-5}	1.171	0.01395	1.040
SF3	3.663×10^{-9}	3.413	4.286×10^{-5}	2.273
SF4	5.817×10^{-5}	1.200	0.00744	1.062
SF5	25.842×10^{-5}	0.954	0.04011	0.780
SF6	14.528×10^{-5}	1.090	0.12381	0.541
SF7	8.804×10^{-5}	1.155	0.08606	0.599
SF8	20.267×10^{-5}	1.017	0.12038	0.549
SF9	3.676×10^{-3}	0.359	0.19220	0.396
SF10	0.1252×10^{-5}	1.999	0.00282	1.266
SF11	6.911×10^{-5}	1.246	0.09159	0.599
SF12	2.164×10^{-5}	1.571	0.00444	1.318
SF13	22.896×10^{-5}	1.084	0.29384	0.412
SF14	4.344×10^{-7}	2.271	0.00401	1.230
SF15	0.1287×10^{-5}	2.137	0.01250	1.048
SF16	1.169×10^{-5}	1.584	0.03197	0.826
SF17	6.694×10^{-5}	1.213	0.02568	0.848
SF18	22.614×10^{-5}	0.986	0.05538	0.710
SF19	N/A	N/A	N/A	N/A

by a changing oxidizer-to-fuel ratio during the combustion event. As expected, SF5, SF6, SF8, and SF11 had similar regression rates.

In contrast to the mass burning rate data, the linear regression rate curve fits tended to have similar characteristics; the exponents were generally less than one. It should be noted that unlike solid propellants, the exponent n or m can exceed unity for hybrid engine applications, since the correlations were associated with oxidizer mass flux rather than pressure.

Figure 7 shows the percentage increase of mass burning rate of the solid fuels compared to HTPB (SF1) interpolated to a single $G_{ox,ave}$ value.

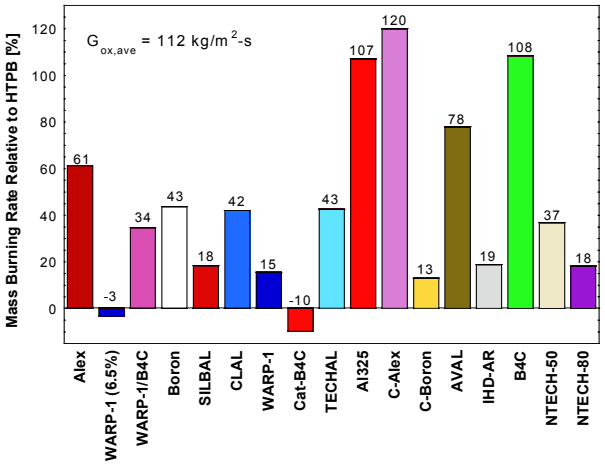

Fig. 7. Percentage increase of mass burning rate of several solid fuel formulations compared to SF1

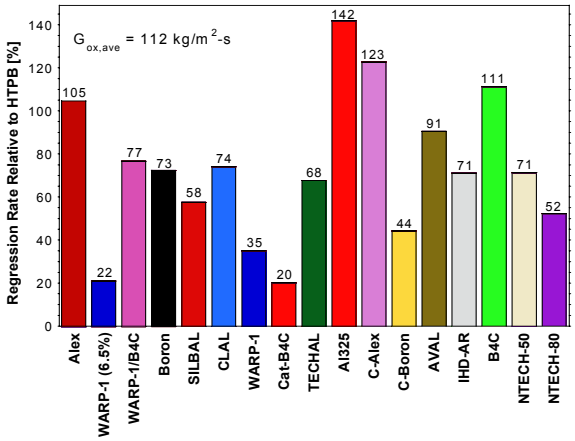

Fig. 8. Percentage increase in linear regression rate of several solid fuel formulations compared to SF1

All (except for SF9 and SF10) solid-fuel formulations containing energetic particles exhibited higher mass burning rates than SF1. Several solid-fuel formulations containing energetic nano-sized particles demonstrated mass burning rates around 42% higher than the baseline formulation at a selected average oxidizer mass flux. Alex®-containing solid fuels indicated the greatest enhancement in mass burning rates of nearly 61%. The solid fuel that contained WARP-1 also demonstrated enhanced mass burning rate compared to SF1 even though the SF4 formulation contained only 6.5% of nano-phase particle loading. Figure 8 shows the comparison between the percentage increase of linear regression rate of nano-particle containing solid fuels and SF1.

C*, Thrust, and Isp Measurements

In rocket propulsion systems, several different empirical parameters are used to determine the relative performance between systems of varying fuels, oxidizers, O/F ratios, etc. These parameters include characteristic velocity (C*), specific impulse (I_{sp}) and thrust (τ). C* is frequently used as a figure of merit for the combustion process and chamber design. It is usually calculated using

$$C^* = \frac{P_c A_{th}}{\dot{m}_p} \tag{5}$$

where,

P_c = chamber pressure [Pa]

A_{th} = nozzle throat area [m^2]

$\dot{m}_p$ = propellant mass flow rate [kg/s]

In a hybrid rocket engine, the propellant mass flow rate is equivalent to the sum of the oxidizer mass flow rate and the fuel mass-burning rate (i.e. $\dot{m}_p = \dot{m}_{tot} = \dot{m}_{ox} + \dot{m}_{fuel}$).

Perhaps the most important parameter in terms of evaluating the chamber geometry and degree of complete combustion is called C* efficiency, which is given by

$$\eta_{C^*} = \frac{C^*_{actual}}{C^*_{theor}} \tag{7}$$

C^*_{actual} corresponds to the characteristic velocity for a specific test run using the measured pressure, fuel mass flow rate, oxidizer mass flow rate, and nozzle throat area. C^*_{theor} represents the ideal (or theoretical) characteristic velocity value at the same conditions. This quantity is commonly obtained using a chemical equilibrium code such as NASA's CEA2000 code.[23]

C Combustion Efficiency*

The C* combustion efficiency of each solid fuel formulation (a better indication of combustion performance) can be seen in Fig. 9. Figure 9 shows the C* combustion efficiency, η_{C^*}, as a function of solid fuel formulation and equivalence ratio.

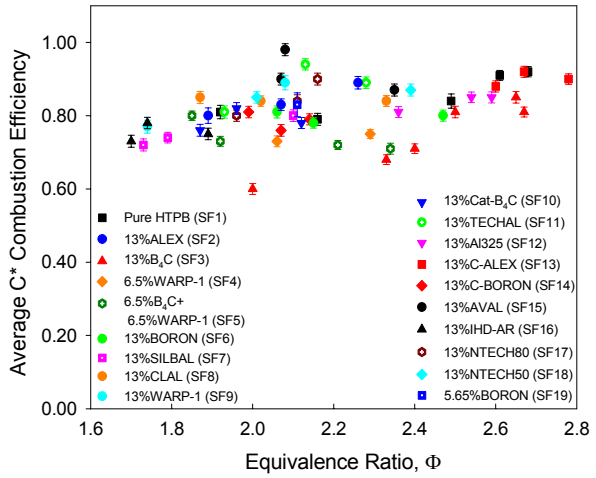

Fig. 9. Average C* combustion efficiency as a function of equivalence ratio

The tests were separated by the solid fuel formulation and were a function of average equivalence ratio. Specifically, at an equivalence ratio of around 2.6, SF13 appeared to be the dominant solid fuel formulation having an average η_{C^*} ranging from 88 to 92%. SF12 (with micron-sized Al particles) exhibited combustion efficiencies from 81 to 85%, which are much lower indicating that the nano-sized particles ignited faster and burned more efficiently to produce large amounts of gaseous products. It is important to note that comparisons between combustion efficiencies of different solid fuel formulations must be performed at very similar equivalence ratios, since theoretical characteristic velocity is strongly dependent on equivalence ratio. Comparing results having different equivalence ratios is misleading.

Described in further detail in a future section is the comparison of mass versus molar variation in particle loading. SF19 consisted of the same amount of boron moles as aluminum moles in other solid fuels. The total number of boron moles was 0.356, which yielded a mass fraction of 0.0565. By comparing SF6 and SF19, it was evident that SF19 has a higher η_{C^*} (83%) than the entire range for SF6 (78 to 81%). This test demonstrated that boron burned more efficiently at lower concentrations in this engine configuration. A summary of solid fuel formulations and their corresponding η_{C^*} ranges is given in Table 5.

Table 5. C* combustion efficiencies (η_{C^*}) for the solid fuel formulations in this study

Solid Fuel	Additive (wt%)	η_{C^*} [%]
SF1	None	72 – 91
SF2	13%Alex®	77 – 89
SF3	13%B_4C	60 – 81
SF4	6.5%WARP-1	73 – 81
SF5	6.5% B_4C/ and 6.5%WARP-1	71 – 80
SF6	13%BORON	78 – 81
SF7	13%SILBAL	72 – 80
SF8	13%CLAL	83 – 85
SF9	13%WARP-1	69 – 89
SF10	13%Cat-B_4C	76 – 82
SF11	13%TECHAL	81 – 94
SF12	13%Al-325	81 – 85
SF13	13%C-Alex	88 – 92
SF14	13%C-Boron	76 – 81
SF15	13%AVAL	87 – 98
SF16	13%IHD-AR	73 – 78
SF17	13%NTECH-80	80 – 90
SF18	13%NTECH-50	76 – 87
SF19	5.65%BORON	83

Instantaneous Thrust Measurements

A typical LGCP thrust trace from a boron-containing solid fuel (SF6) is shown in Fig. 10. In the figure, the maximum thrust achieved is around 130 N. All of the thrust traces obtained using the LGCP rocket engine had the same basic characteristics. A small thrust level was generated by the onset of the oxidizer flow and then ignition caused a rapid rise in thrust. After ignition, a steady-state profile was established; nearly constant thrust was achieved.

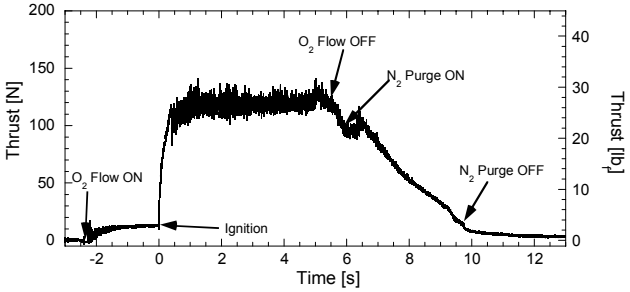

Fig. 10. Typical thrust trace of LGCP motor firing (NS-41)

Immediately after the oxidizer was shut off, the nitrogen purge was activated. Finally, the last slight decrease in thrust (at around 10 seconds) was due to the nitrogen purge being shut off. Figure 11 illustrated the average thrust for all of the tests conducted as a function of solid fuel formulation and average oxidizer mass flux. The parameters were time-averaged from the onset of ignition to onset of the nitrogen purge. SF13 (13%C-Alex) produced the highest amount of thrust which was a result of high mass and linear burning rates.

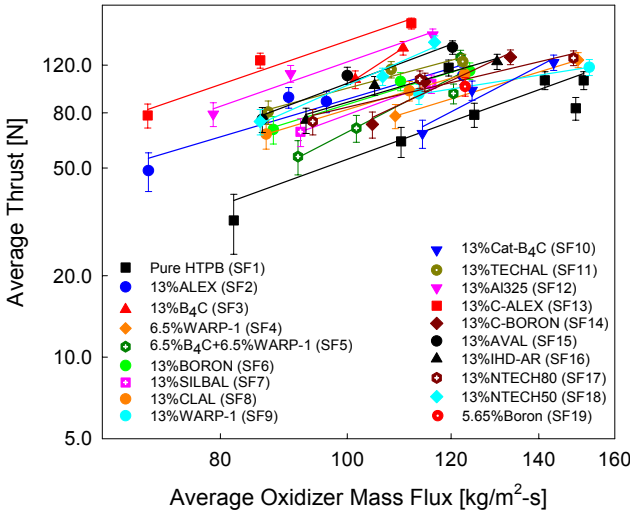

Fig. 11. Average thrust as a function of average oxidizer mass flux

Another factor in thrust production was the nozzle expansion ratio. The expansion ratio, ε, was approximately 5 for the tests conducted in this investigation which may not be an optimum ratio.

Specific Impulse

I_{sp} is a measure of the amount of thrust obtained by combusting a unit weight of fuel and oxidizer (or propellant) at Earth standard conditions. It was calculated by the following

$$I_{sp} = \frac{\tau}{\dot{m}_p g} \tag{6}$$

where,

τ = thrust [N]

g = gravitational constant [9.81 m/s^2]

Specific impulse, I_{sp}, is a conventional measure of the performance of full-scale rockets. However, for lab-scale rockets, the absolute specific impulse value obtained may be misleading. Several factors in lab-scale specific impulse measurements contribute to errors in the measurements such as nozzle contour, expansion ratio, thrust variation, and overall scale of the system. The merit of calculating specific impulse in such small motors is to compare various solid fuel formulations or oxidizers to each other using the same rocket engine. In this study, I_{sp} was used as a qualitative tool to evaluate the relative specific impulse performance among a family of solid fuel formulations. In addition to I_{sp}, specific impulse efficiency (η_{Isp}) was also determined to compare the empirical I_{sp} values to ideal theoretical calculations. Specific impulse efficiency was calculated in a similar manner to C* combustion efficiency and is given by

$$\eta_{Isp} = \frac{Isp_{actual}}{Isp_{theor}} \tag{8}$$

Isp_{actual} is the specific impulse for a test run using the measured pressure, fuel mass flow rate, oxidizer mass flow rate, nozzle expansion ratio, and nozzle throat area. Isp_{theor} represents the ideal (or theoretical) specific impulse value at the same conditions. This quantity is commonly obtained using a chemical equilibrium code such as NASA's CEA2000 code.[23] Figure 12 shows the average I_{sp} for several solid fuel formulations as a function of equivalence ratio.

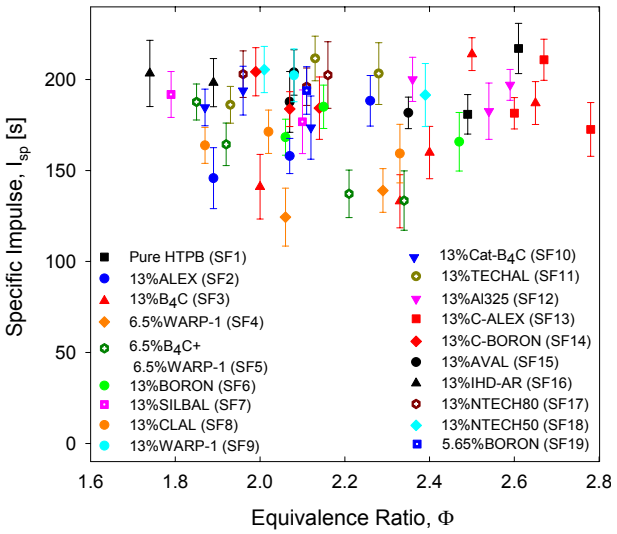

Fig. 12. Average specific impulse, I_{sp}, as a function of equivalence ratio

The general trend for the data points shown in the figure seemed to be fairly constant, ranging from 150 to 200 seconds, which was below full-scale results. The specific impulse trends mimic the trends found in the thrust data since the specific impulse was directly calculated using the measured thrust. Figure 13 shows the specific impulse efficiency of the solid fuel

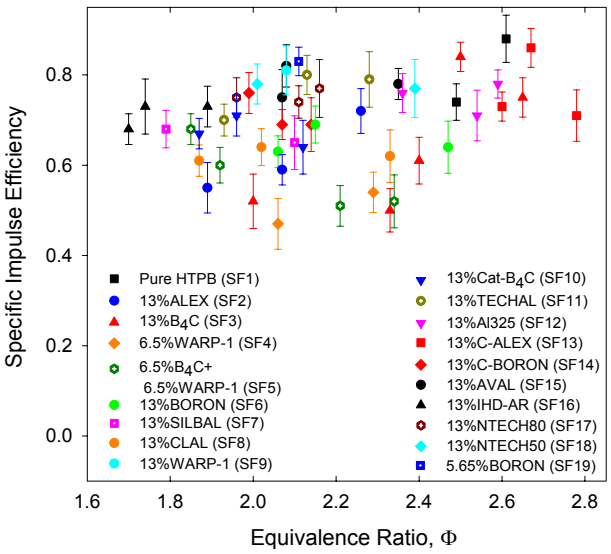

Fig. 13. Average specific impulse efficiency, η_{Isp}, as a function of equivalence ratio

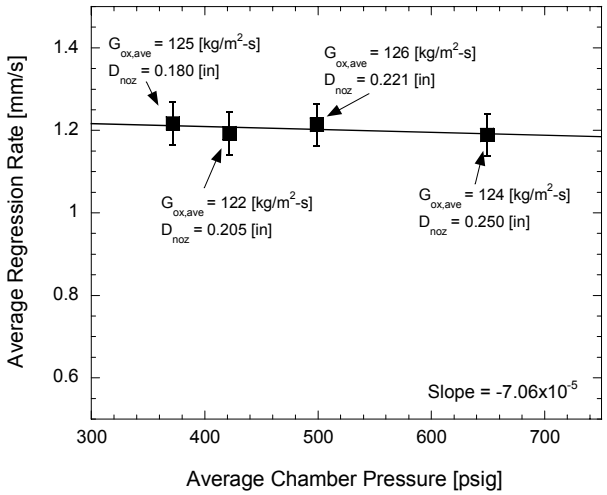

Fig. 14. Effect of chamber pressure on average regression rate

formulations. The maximum η_{Isp} was approximately 86%, which corresponded to SF13. This was consistent since SF13 produced the largest amount of thrust.

Chamber Pressure Effect

The hybrid-engine combustion model, developed by Marxman and coworkers[24,25,26] was based on turbulent boundary-layer transport mechanisms with diffusion-limited combustion process. As a result, this model predicted that the regression rate, r_b, of the solid fuel surface was independent of pressure above a certain threshhold. Four tests were conducted at various pressures while holding the average oxidizer mass flux constant. The pressure in the rocket engine was regulated by substituting various graphite nozzles with different nozzle throat diameters for each test. For this series of tests, the average oxidizer mass flux was 125 kg/m^2-s, the nozzle throat diameters were 0.457 (0.180), 0.521 (0.205), 0.561 (0.221), and 0.635 (0.250 in) centimeters. These nozzle diameters regulated the average chamber pressures to 2.67 MPa (386.7 psia), 3.01 (436.7), 3.54 (513.7), and 4.58 (663.7), respectively. Experimental evidence obtained in this investigation proved that the linear regression rate was independent of pressure from the range from 2.51 to 4.58 MPa (364.7 to 664.7 psia) as shown in Fig. 14. This reinforces that the pyrolysis and combustion processes of solid fuels used in hybrid rocket engines are diffusion-controlled not kinetically-controlled like most solid propellants.

Volumetric versus Gravimetric Loading of Particles

From hybrid rocket experiments, it was obvious that boron-containing solid fuel formulations produced plume jets that contained copious amounts of luminous partially-burned particles. Unburned particles in the exhaust plume indicated that a portion of the heat release produced by particle combustion occurred in the exhaust of the rocket engine rather than in the combustion chamber. This was undesirable from a combustion efficiency standpoint. Carrying particles on board the rocket without fully combusting them to generate hot gases which, in turn, produce thrust, is a waste of payload.

Conventionally, the mass fractions of ingredients are varied to achieve maximum performance. To achieve the same mass fraction of aluminum (Y_{Al} = 0.13), roughly three times the amount of boron atoms was required since the molecular weight is three times smaller. From a chemical point of view, it would be more difficult to fully burn all of the boron particles if the oxygen delivered to the combustion zone is constant since the concentration is much higher. Therefore, tests were conducted at equal molar amounts of boron and aluminum. The HTPB, aluminum, and ingredients were assumed to pyrolyze to form product gases so that gas-mixture equations can be used. Therefore, SF19 contained 5.65% boron (by weight) to investigate the effect of molar equivalency at an average oxidizer mass flux of 125 kg/m^2-s. SF6 contained 13% boron (by weight). A significant amount of large luminous particles were visible in the exhaust plume indicating that the combustion was not complete or the residence time of the engine was too short. Also, this implied that all of the potential heat generated from the combustion

of the energetic particles was not released in the chamber, but in the exhaust plume. Post-test calculations showed the combustion efficiency of solid fuels containing 13%boron was low (~79%).

Figure 15 shows a captured image of a plume jet of SF19. As one can see, the lower concentration of boron affected the characteristics of the plume which contained very few luminous particles. In contrast, tests conducted using SF6 showed significant amounts of visible particles in the exhaust plume. This observation coincided with the low C* combustion efficiency calculated for this test. Furthermore, the combustion efficiency (η_{C^*} = 0.83) for the SF19 was higher for the same oxidizer mass flux of 125 kg/m^2-s.

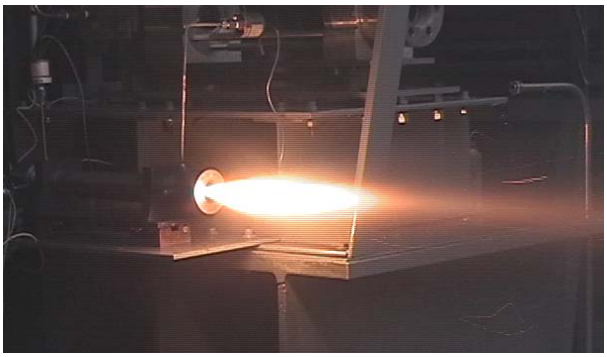

Fig. 15. Captured image of the exhaust plume for SF19

CONCLUSIONS

Several interesting observations can be drawn:

1. Formulations containing nano-sized energetic particles showed significant performance enhancement compared to pure HTPB (SF1) with the highest having nearly 120% increase in mass burning rate for a 13% Viton-A coated Alex® powder an oxidizer mass flux of 112 kg/m^2-s, and even greater for larger oxidizer mass fluxes. This increase was due to the enhanced heat transfer rate caused by the combustion of nano-sized particles at the close vicinity of the burning surface. Based upon engineering analysis, the ignition and burning times of a 100-nm particle was on the order of a few nanoseconds which allowed the particle to fully release the energy during combustion inside of the combustion chamber in the close vicinity of the surface thereby increasing heat transfer.
2. The decomposition of a fluoropolymer coating provided additional oxidizer to react with aluminum near the surface of nano-sized particles to enhance ignition. Results show a 123% increase in regression rate for coated Alex® powder at the same oxidizer mass flux. Solid fuel (SF8) with Viton-A coated aluminum flakes (CLAL) showed a mass burning rate twice as high as the solid fuel (SF7) with uncoated aluminum flakes (SILBAL).
3. In terms of percentage increase in linear regression rate, SF4 (with 6.5%B_4C and 6.5%WARP-1), SF6 (with 13%BORON), SF8 (with 13%CLAL), and SF11 (with 13%TECHAL) all demonstrate an increase of at least 68% compared to SF1 (100%HTPB) because of the greater energy release by nano-sized particle oxidation near the surface.
4. Boron-containing solid fuels (13% by weight) exhibited lower C* combustion efficiencies (ranging from 78 to 81%) compared to aluminum-containing fuels. Moreover, boron-carbide (B_4C)-containing fuels demonstrated the lowest C* combustion efficiencies, ranging from 61 to 81%.
5. The maximum η_{Isp} for a solid fuel containing energetic particles was approximately 86%, which corresponded to SF13. This was consistent since SF13 produced the largest amount of thrust among the metallized solid fuels. Boron-containing solid fuels also exhibited lower I_{sp} efficiencies (ranging from 62 to 69%) compared to aluminum-containing fuels. Moreover, boron-carbide (B_4C)-containing fuels demonstrated the lowest I_{sp} efficiencies, ranging from 50 to 60%.
6. SF13 demonstrated the highest thrust levels (ranging from 80 to 130 N for various average oxidizer mass fluxes) among all of the solid fuel formulations. SF1 (pure HTPB with no energetic particles) exhibited the lowest thrust levels (around 25 to 80 N) for the same oxidizer mass flux range.
7. SF13 demonstrated a 171% increase in thrust compared to the baseline solid fuel (SF1) for an average oxidizer mass flux of 112 kg/m^2-s. Both B_4C-containing solid fuels (SF3 and SF10) showed minimal increases in thrust (3% and 5%, respectively) compared to SF1.
8. Tests were conducted while keeping the molar content constant between aluminum-containing and boron-containing solid fuels. Using molar equivalence, solid fuels that contained 13% aluminum (by weight) correspond to 5.65% boron (by weight). Test results indicated that SF19 (5.65% boron) exhibited a higher C* combustion efficiency (83%) compared to SF6 (13% boron) at an average oxidizer mass flux of 125 kg/m^2-s. Unlike tests conducted using SF6, no luminous particles were observed in the exhaust plume of SF19 implying that the limiting factor may be mixing and/or oxidizer availability to the particles.
9. Solid fuel containing various types of nano-sized aluminum particles showed some differing results despite the fact that fuel formulations are identical. Some of the factors which can contribute to this difference include: particle size distribution,

specific surface area, active aluminum content, impurity content, and spheriosity of the particles.

FUTURE WORK

1. Investigate the effect of varying energetic additive percentages in the solid fuel on the C* combustion efficiency and thrust generation.
2. Examine the combustion behavior of fuels/propellants containing nano-particles of different energetic materials such as: Mg, Ti, etc., coating of particles, polymers or other metal layer to enhance ignition and other properties, intermetallic/reactive particles, or hydrides to generate hydrogen gas from decomposition.
3. Perform more extensive chemical analyses on both virgin and recovered solid fuel grains to quantify the composition of the quenched layer.
4. Investigate various cross-linking agents to improve solid fuel integrity and to increase the working time of the uncured solid fuel during processing.
5. Examine the suitability of several liquid oxidizers (such as HAN-based or HAP-based liquids or H_2O_2) in hybrid rocket applications.
6. Process new families of HTPB-based solid fuel grains with multiple types of metal additives in a single solid-fuel grain.

ACKNOWLEDGEMENTS

The authors would like to thank the Naval Surface Warfare Center-Indian Head Division of the Department of the Navy for the sponsorship of this SBIR program through the Combustion Propulsion and Ballistic Technology Corporation under the contract number N00174-02-M-0114 with a subcontract to PSU. The support and encouragement from Mr. Carl Gotzmer and Mrs. Nancy Johnson are greatly appreciated. The donation of nano-particles from Mr. Fred Tepper of the Argonide Corporation, Dr. May Chan of NAWC-China Lake, Dr. Gary Pozarnsky of Aveka, Inc., Dr. Denny Hamill of Nanotechnologies, Inc., and Dr. David Pesiri of Technanogy is greatly acknowledged. The authors would also like to acknowledge Dr. Curtis E. Johnson of NAWC-China Lake for his effort in determining the active aluminum content in different nano-sized particles. The assistance of Dr. Abdullah Ulas and Mr. Surajit Kumar in the earlier part of this study is greatly appreciated. Special thanks goes to Mr. Peter J. Ferrara for his help with nozzle and mandrel plug fabrication. The efforts of Nick Favorito are also acknowledged. The advice and council of Dr. Natan Libis is appreciated.

REFERENCES

[1] Sutton, G. P., *Rocket Propulsion Elements: An Introduction to the Engineering of Rockets*, 6th Edition, John Wiley and Sons, Inc., 1992.

[2] Altman, D., "Hybrid Rocket Development History," AIAA Paper No. 91-2515, 27th AIAA/SAE/ASME/ ASEE Joint Propulsion Conference, Sacramento, CA, June 24-26, 1991.

[3] Kuo, K. K., "Importance and Challenges of Hybrid Rocket Propulsion Beyond Year 2000," Invited von Kármán Lecture in the Proceedings of the 37th Israel Annual Conference on Aerospace Sciences, pp. II-1 to II-31, February 26-28, 1997.

[4] Chiaverini, M. J., Serin, N., Johnson, D., Lu, Y. C., Kuo, K. K., and Risha, G. A., "Regression Rate Behavior of Hybrid Rocket Solid Fuels," *Journal of Propulsion and Power,* Vol 16, No. 1, pp. 125-132.

[5] Strand, L. D., Ray, R. L., Anderson, F. A., and Cohen, N. S., "Hybrid Rocket Fuel Combustion and Regression Rate Study," AIAA Paper 92-3302, June 1992.

[6] Teague, W., Wright, A., Balkanli, D., and Hybl, L, "Effect of Energetic Fuel Additives on the Temperature of Hybrid Rocket Combustion," AIAA 99-2138, June 1999.

[7] Pranda P., Prandova K. and Hlavacek V., "Particle Size and Reactivity of Aluminum Powders", *Combustion Science and Technology*, Vol 156, pp 81-96, 2000.

[8] Ivanov, G., "Uniformity of Burning and Detonation of Pyrotechnic Mixtures Based on Activated Aluminum," 1995 JANNAF Propulsion Meeting CPIA Pub. 630, Vol. 1, 1995, pp. 89-95.

[9] Chiaverini, M.J., Serin, N., Johnson, D. K., Lu, Y.C., and Kuo, K.K, "Instantaneous Regression Behavior of HTPB Solid Fuels Burning with GOX in a Simulated Hybrid Rocket Motor," Challenges in Propellants and Combustion 100 Years After Nobel, edited by K.K. Kuo, Begell House, Inc., New York, 1997, pp. 719-733.

[10] Chiaverini, M. J., Kuo, K. K., Peretz, A., Harting, G. C., "Regression Rate and Heat-Transfer Correlations for Hybrid Rocket Combustion," *Journal of Propulsion and Power,* Vol 17, No. 1, pp. 99-110.

[11] Mench, M. M., Yeh, C. L., and Kuo, K. K., "Propellant Burning Rate Enhancement and Thermal Behavior of Ultra-fine Aluminum Powders," Energetic Materials Production, Processing and Characterization, 29th International ICT Conference, June 30 - July 3, 1998, pp 3-01-3-05.

[12] Li, S. and Jin, R., "Improvement of Combustion Characteristics of Solid Propellant with Coated Boron," AIAA Paper No. 99-2633, 35th AIAA/ASME/SAE/ASEE Joint Propulsion Conference, Los Angeles, California, June 20-24, 1999.

[13] Shyu, I-M. and Liu, T-K., "Combustion Characteristics of GAP-Coated Boron Particles and the Fuel-Rich Solid Propellant," *Journal of Combustion and Flame,* The Combustion Institute, Pittsburgh, 1995, Vol 100, pp. 634-644.

[14] Liu, T. K., Luh, S. P., and Perng, H. C., "Effect of Boron Particle Surface Coating on Combustion of Solid Propellants for Ducted Rockets," Propellants, Explosives, Pyrotechnics, Vol 16, pp 156-166, 1991.

[15] Personal communication with Dr. May Chan of NAWC-China Lake.

[16] Risha, G. A., Harting, G. C., Kuo, K. K., Peretz, A., and Koch, D. E., "Pyrolysis and Combustion of Solid Fuels in Various Oxidizing Environments," AIAA Paper No. 98-3184, 34th AIAA/ASME/SAE/ASEE Joint Propulsion Conference, Cleveland, OH, July 13-15, 1998.

[17] Risha, G. A., Ulas, A., Boyer, E., Kumar, S., and Kuo, K. K., "Combustion of HTPB-Based Solid Fuels Containing Nano-Sized Energetic Powder in a Hybrid Rocket Motor," 37th AIAA/ ASME/ SAE/ ASEE JPC in Salt Lake City, Utah, AIAA Paper No. 2001-3535, July 2001.

[18] Risha, G. A., Boyer, E., Wehrman, R. B., and Kuo, K. K., "Performance Comparison of HTPB-Based Solid Fuels Containing Nano-Sized Energetic Powder in a Cylindrical Hybrid Rocket Motor," 38th AIAA/ ASME/ SAE/ ASEE JPC in Indianapolis, Indiana, AIAA Paper No. 2002-3576, July 2002.

[19] Johnson, C. E., and Higa, K. T., "Preparation of Nanometer Sized Aluminum Powders," the Proceedings of the 1997 JANNAF Propellant Development and Characterization Subcommittee, and the Safety and Environmental Protection Subcommittee Joint Meeting, CPIA-Pub-647-Vol-I, pp 137-142, March 1997.

[20] Personal communication with Dr. Curtis C. Johnson of NAWC, China Lake. 2002.

[21] Personal communication with a Silberline representative, June 1999.

[22] Risha, G. A. "Enhancement of Hybrid Rocket Combustion Performance Using Nano-Sized Energetic Particles," Ph.D. Dissertation, August 2003.

[23] Mcbride, B. J. and Gordon, S., "Computer Program for Calculation of Complex Chemical Equilibrium Compositions and Applications," NASA Reference Publication 1311, June 1996.

[24] Marxman, G.A., and Gilbert, M., "Turbulent Boundary Layer Combustion in the Hybrid Rocket," *Ninth Symposium (International) on Combustion*, Academic Press, Inc., New York, 1963, pp. 371-383.

[25] Marxman, G.A., Wooldrige, C.E., and Muzzy, R.J., "Fundamentals of Hybrid Boundary-Layer Combustion," *Heterogeneous Combustion*, edited by H.G. Wolfhord, I. Glassman, and L. Green, J., Vol. 15, Progress in Astronautics and Aeronautics, Academic Press Inc., New York, 1964, pp.485-522.

[26] Marxman, G.A., "Combustion in the Turbulent Boundary Layer on a Vaporizing Surface," *Tenth Symposium (International) on Combustion*, The Combustion Institute, Pittsburgh, 1965, pp. 1337-1349.